On Error and Bitrate Tradeoff in Visible Light Communication System to ensure HEVC Video Quality

Hamed Alizadeh Ghazijahani
Faculty of Electrical and Computer Engineering,
University of Tabriz, Tabriz, Iran
hag@tabrizu.ac.ir

Milad Abdollahzadeh
Faculty of Electrical and Computer Engineering,
University of Tabriz, Tabriz, Iran
milad.abdollahzadeh @tabrizu.ac.ir

Hadi Seyedarabi
Faculty of Electrical and Computer Engineering,
University of Tabriz, Tabriz, Iran
seyedarabi @tabrizu.ac.ir

Mir Javad Musevi Niya
Faculty of Electrical and Computer Engineering,
University of Tabriz, Tabriz, Iran
niya @tabrizu.ac.ir

Abstract— **Recently, Visible Light Communication (VLC) has got increasing attention in the field of indoor wireless communications. Color Shift Keying (CSK) is a VLC modulation scheme proposed by IEEE 802.15.7 task group. In this method diffused light wavelengths are symbol points so that their combination provides an overall white sensation. Modulation depth in CSK influences Bit Error Rate (BER) as determines transmission rate. In the case of video streaming over VLC network, video encoding rate should be compatible with the transmission rate, consequently, affects video quality. We have proposed an adaptive modulation scheme for video transmission over VLC network considering the dependency of encoded video quality and modulation BER to modulation. This algorithm jointly minimizes BER and encoded video distortion via adaptive selection of CSK modulation depth to decline frame loss besides desirable video quality protection.**

Keywords- bit error rate; color shift keying; modulation; video streaming; visible light communication.

I. INTRODUCTION

In recent years demands for wireless data communication has increasing growth. This leads to congestion in radio frequency spectrum. To overcome this phenomenon, researchers focused on optical communication systems. Visible Light Communication (VLC) is one of the attractive optical communication systems that utilizes visible region of the optical spectrum with the advantage that this band is unregulated [1-5]. Intensity modulation with direct detection (IM/DD) is typically used in VLC systems because of its simplicity [6]. Higher data rates are achievable thanks to Light Emitting Diodes (LEDs) with fast nanosecond switching time capability [1, 3, 4]. The human visual system does not recognize LED flicker to at least 50 Hz [7]. Therefore, communication and illumination can be used simultaneously.

The first standard for VLC has developed in 2011 by IEEE 802.15.7 task group with the definition of three physical layers namely PHY I, PHY II and PHY III [2, 8]. Color Shift Keying (CSK) is a manner considered as a modulation scheme for indoor applications (PHY III) [8] which utilizes Red (R), Green (g) and Blue (B) LEDs. The aforementioned standard determines

different light wavelengths as symbol points. These wavelengths are chosen in a way that equal occurrence probability results in white color [9].

Higher data rates of VLC can be useful in several indoor application scenarios such as: video transmission for video conference, real-time monitoring, and video on demand [10]. Digital video is bulky data with high amount of redundancy. Therefore, in most applications video data are compressed before transmission. Several video coding standards have been proposed for this task.

High Efficiency Video Coding (HEVC) standard is the most recent joint video project of the ITU-T Video Coding Experts Group (VCEG) and the ISO/IEC Moving Picture Experts Group (MPEG) standardization organizations, working together in a partnership known as the Joint Collaborative Team on Video Coding (JCT-VC) [11]. The fundamental goal of the HEVC is the fact that presents considerably better compression performance in comparison with the current existing standards for about the same video quality. Moreover, it is designed to provide high-quality streaming media, even on low-bandwidth networks [12]. Therefore, there are many benefits of using HEVC compression standard for media files compared to other standards [13].

In video transmission over VLC network, modulation depth in CSK determines transmission rate which dictates video encoder rate and accordingly video quality. Moreover, modulation depth affects Bit Error Rate (BER). Because of higher importance of header bits in video data packets, a single bit error may cause frame loss. Therefore, in higher BER, the probability of frame loss will increase. Consequently, a tradeoff between video quality and frame loss probability should be considered. In this work, proper choose of modulation depth balances this tradeoff. Frame loss has been modeled based on BER and sensitivity of header bits of HEVC bitstream to bit errors. On the other hand, video quality is related to encoder rate via rate-distortion model of HEVC encoder. We use these relations to jointly optimize video quality and frame loss by choosing proper CSK modulation depth.

Contributions of this work are as follows:

- An adaptive modulation depth selection for CSK modulation is proposed. This method aims to minimize both video distortion and frame loss in a given SNR.
- In order to estimate the frame loss probability of a video sequence, we have calculated the BER of CSK modulation as a function of SNR.
- Furthermore, considering HEVC as video encoder, we have proposed an accurate rate-distortion model for HEVC video encoder.
- Finally, two major encoding methods of HEVC encoder namely Intra- and Inter-mode are compared based on the proposed method and some guidelines are provided to choose

appropriate encoding mode in the given SNR.

The rest of paper is organized as follows. Section II explains basics of CSK modulation. Proposed algorithm for video transmission over VLC is stated in section III. Section IV describes results and discussion. The paper is concluded in section V.

II. CSK BASICS

IEEE 802.15.7 standard supports the three physical layer types, i.e. PHY I, PHY II and PHY III [14]. The PHY I and PHY II are intended for outdoor usage with low and moderate data rate applications. These support OOK and VPPM modulation schemes, respectively. The PHY III uses CSK modulation for data communication rates in tens of Mbps [8, 15].

In CSK, the transmitter utilizes three LED with a specific set of wavelengths related to red, green and blue colors. The CSK constellation definition is based on the x-y color coordinates of CIE 1931 color space standard and each symbol is represented by a unique color. A color space is a notation by which we can specify colors, i.e., the human perception of the visible electromagnetic spectrum. Various color spaces can be used to represent the colors of the visible spectrum, such as RGB. The tristimulus values are the amount of the three primary colors in a three component additive color model needed to generate a target color, denoted by X, Y, and Z, which are given by $X = \int S(\lambda) \bar{x}(\lambda) d\lambda$, $Y = \int S(\lambda) \bar{y}(\lambda) d\lambda$ and $Z = \int S(\lambda) \bar{z}(\lambda) d\lambda$, where λ is the wavelength (in nanometers) of the monochromatic light equivalent to each primary color. $\bar{x}(\lambda)$, $\bar{y}(\lambda)$ and $\bar{z}(\lambda)$ are three color matching functions used in the CIE 1931 color space, and $S(\lambda)$ is spectral power distribution of a light source. Three tristimulus values can be normalized by the following equations:
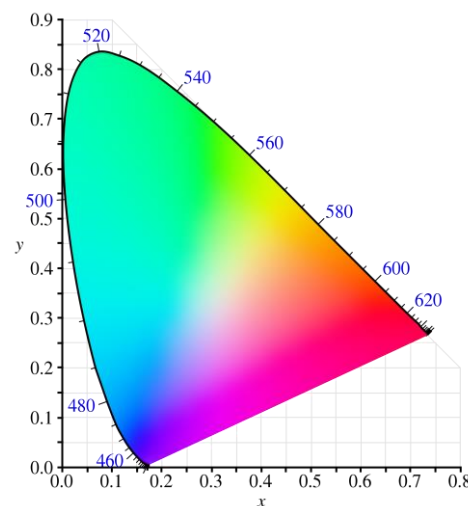
$$x = \frac{X}{X + Y + Z}$$
$$y = \frac{Y}{X + Y + Z}$$

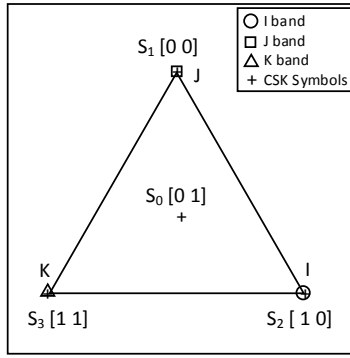
Fig. 1. CIE 1931 color space chromaticity diagram

Fig. 2. Constellation and data mapping for 4-CSK.

$$z = \frac{Z}{X + Y + Z}$$

$$x + y + z = 1 \qquad (1)$$

Using these normalized values, a chromaticity diagram, known as the CIE 1931 color space chromaticity diagram can be drawn. The vertical projection onto the xy-plane of the chromaticity diagram is shown in Fig. 1. All visible colors differ only by luminance map to the same point in the chromaticity diagram [16].

The transceiver mechanism is based on the IM/DD. The IEEE 802.15.7 CSK physical layer standard specifies all the possible colors namely Color Band Combinations (CBC). Fig. 2 shows the constellation diagram for 4-CSK. The mean chromaticity of I, J and K bands results in white color, which is the target color for ambient lighting.

The block diagram of the uncoded CSK system is depicted in Fig. 3. In this system, the data is mapped to the relevant symbol on the CIE 1931 diagram. Then the chromaticity of the symbol is analyzed to the color intensities. The following set of equations shows this process.

$$x = P_i x_i + P_j x_j + P_k x_k \qquad (2)$$

$$y = P_i y_i + P_j y_j + P_k y_k \qquad (3)$$

$$P_i + P_j + P_k = 1 \qquad (4)$$

where (x_i, y_i) , (x_j, y_j) and (x_k, y_k) are the chromaticity values at the central wavelengths of the three sources (LEDs), respectively. These color points are generated by the intensity of three light sources P_i, P_j and P_k [17, 18].

In this system, dimming is done by multiplying the intensities of source feeders to the arbitrary value, namely dimming factor g_d, typically between 10-100 percent [4]. In general, (3) can be written as below:

$$g_d P_i + g_d P_j + g_d P_k = g_d \qquad (5)$$

$$\int_{kT_s}^{(k+1)T_s}(g_d P_i + g_d P_j + g_d P_k)dt = g_d T_s \qquad (6)$$

where T_s is the time interval of a symbol. Such a dimming scheme reduces the overall signal energy. Consequently, performance of the system reduced for small dimming factors in terms of symbol error rate (SER).

III.   PROPOSED ALGORITHM

As described, the VLC system has the obligation of lighting besides data communication. In this regard, any VLC system should have the capability of dimming to adjust indoor light intensity. Different dimming schemes are proposed in literature but in all of them the overall power of R, G and B LEDs are controlled to have desired light intensity. Dimming will effect on Signal to Noise Ratio (SNR) of received signal, monotonically.

The decrease in SNR results in an increase of BER which gains Frame Loss Rate (FLR). In the case of video applications, quality of experience includes both temporal and spatial quality. Temporal quality is achievable with successful decoding of video frames regardless of its content. However, spatial quality considers the quality of reconstructed data within each frame. A Higher value of FLR degrades users' temporal quality drastically which makes video transmission useless. Therefore, in order to have an acceptable temporal quality, it is essential to decrease modulation depth to reduce FLR. On the other hand, decreasing modulation depth results in decreasing video encoder rate and accordingly decrease in spatial video quality. So there is a tradeoff between delivered video quality and FLR. Similarly, increasing SNR results in lower BER. If we use the same modulation depth, the opportunity of higher spatial video quality will be lost. Therefore, both video quality and FLR should be considered to choose proper modulation depth.

Proposed algorithm uses mathematical modeling to jointly optimize FLR and video quality. This model besides adaptive CSK modulation results in choose of a proper modulation depth for different SNR values.

A. CSK Modulation BER Analysis

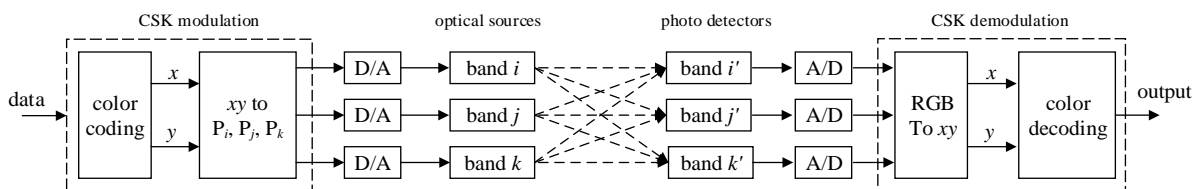The IEEE 802.15.7 standard has defined different

Fig. 3. Uncoded CSK system.

CBCs for 4, 8 and 16-ary CSK modulation. The BER of CSK modulation for all the three depths should be calculated versus different SNRs to be considered besides video quality model.

To investigate the performance of the M-ary CSK modulation analytically, we assume that the electronic noise, together with background noise, is the dominant noise source and is modeled by AWGN that is statistically independent between time slots [19]. Following the union-bound-based approach for driving an upper bound for average SER, it is calculated as [20-22]:

$$P_{e,union} = \sum_{m=1}^{M} \sum_{\substack{n=1 \\ n \neq m}}^{M} p_m P(\hat{s}^{(m)} \rightarrow s^{(n)})$$

$$\sum_{m=1}^{M} \sum_{\substack{n=1 \\ n \neq m}}^{M} p_m Q\left(\sqrt{\frac{d_{nm}^2}{2N_0}}\right)$$

$$= \frac{1}{M} \sum_{m=1}^{M} \sum_{\substack{n=1 \\ n \neq m}}^{M} Q\left(\sqrt{\frac{d_{nm}^2}{2N_0}}\right) \qquad (7)$$

with p_m representing the m-th symbol transmission probability, M is the constellation size (Modulation depth), here $M = 4, 8, 16$, $Q(t) = 1/\sqrt{2\pi} \int_x^\infty exp(-t^2/2)dt$ is the Gaussian tail error probability and d_{nm}, the Euclidean distance between any pair of signal points is

$$d_{nm} = \sqrt{\|I_n - I_m\|^2}$$
$$d_{nm} = \sqrt{\left(\sum_{j=1}^{l}(I_{n,j} - I_{m,j})^2\right)} \qquad (8)$$

where l is the dimension of constellation. Considering R, G and B channels, gives $l = 3$. Fig. 4 depicts the analytical results of BER upper bound for $M = 4, 8, 16$.

B. HEVC Video Characteristics

High Efficiency Video Coding, also known as H.265, is a new video compression standard. HEVC was developed with the goal of providing twice compression efficiency of the previous standard, H.264/AVC. Although compression efficiency results vary depending on the type of content and the encoder settings, at typical consumer video distribution bit rates HEVC is typically able to compress video twice as efficiently as H.264/AVC.

In predictive video coding standards like HEVC, various bits of output bitstream packets have different importance in video reconstruction. This yields different sensitivity levels to bit errors in the bitstream. Header bits of a coded video packet play most important rule in video reconstruction which makes them more vulnerable to bit errors. A single error in header bits has the potential to discard the whole frame. With this in mind, a simple upper bound probability for

frame loss probability of HEVC encoder can be modeled as:

$$p_{FL} = \frac{N_H}{N_T} \times BER \qquad (9)$$

where p_{FL}, N_H and N_T denotes frame loss probability, average number of header bits of each frame and average number of total bits of each frame, respectively.

As mentioned before, modulation depth determines encoder rate which affects spatial video quality. Therefore, choosing modulation depth without considering encoding algorithm results in quality degradation of reconstructed video. In order to prevent this fault, it is essential to know the relation between bitrate and quality of video encoder. There are some models addresses this issue. Recently Li, et al. [5] discovers the relation between rate and distortion for HEVC encoder. They use a Hyperbolic function to model this relation as (8).

$$D(R) = \alpha R^{-\beta} \qquad (10)$$

With D and R represents distortion and rate of encoded video, respectively. Additionally, α and β are model parameters which obtained by linear regression. A Higher value of D means lower spatial video quality and vice versa. In our previous work [23], we investigate that adding an additional term to (10) will improve the accuracy of this model. Equation (11) represents modified model:

$$D(R) = \alpha R^{-\beta} + c \qquad (11)$$

Similarly, α, β, and c are content dependent model parameters which obtained by linear regression. Fig. 5 demonstrates the higher accuracy of proposed model for "Race Horses" video sequence. Using R-square as fitting metric, in average Li and proposed models result in 0.9843 and 0.9997 respectively [24].

C. Modulation Depth Selection Scheme

As Fig. 4 indicates, the BER is related to modulation depth, M, in a sense that for a specific SNR value, increasing M results in higher BER. Additionally, the frame loss probability of HEVC codec is related to the BER in (9). Therefore, frame loss probability of HEVC
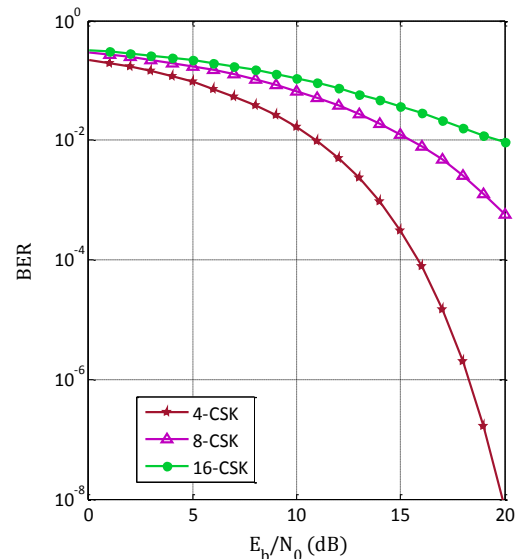

Fig. 4. Analytical results of BER for $M = 4, 8, 16$.

encoded video is dependent to *M*. On the other hand, modulation depth enforces encoder rate which is related to video quality by (11) for HEVC encoded video. Thus, the video quality of HEVC video is dependent on *M*. Using this model, modulation depth determines both frame loss probability and video quality for HEVC video.

As mentioned, there is a tradeoff between FLR and video quality in which proper choose of *M* can balance it. In order to jointly minimize frame loss probability and video distortion we define following cost function:

$$CF = \theta_1 D + \theta_2 FL \quad (12)$$

where, *CF*, *D,* and *FL* stands for cost function, video distortion and frame loss probability, respectively. Also, θ_1 and θ_2 are constant parameters depending on video data. For $M = 4, 8, 16$, the CF is derived as below:

$$CF_M = \theta_1\left(\alpha R_M^{-\beta} + c\right) + \theta_2\left(\frac{N_H}{N_T} \times BER_M\right),$$
$$M = 4, 8, 16 \quad (13)$$

The *CF* is varied versus SNR for various values of *M*, distinctly. For different values of SNR, the modulation depth with a minimum value of *CF* is chosen. Considering that the components of CF_M are SNR dependent, for different SNR intervals, distinct M satisfies minimum values of frame loss and distortion. SNR interval boundaries for utilizing different M's will be obtained by cross points of three *CF* curves. We have used different video sequences with different characteristics namely "Bus", "City" and "Race Horses" to analyze proposed scheme. A prominent feature of "Bus" sequence is high motions while "Race Horses" sequence contains slow motion with higher details. Additionally, in "City" sequence there is quick motion with higher details.

Fig. 6 illustrates logarithmic *CF* value of HEVC encoded "Bus" video sequence for M = 4, 8 and 16 versus SNR. According to cross points in Fig. 6, the proper modulation scheme for SNRs below 12.6 is 4-CSK, for 12.6 < SNR ≤ 17.2 is 8-CSK and SNRs over 17.2, 16-CSK is the best. Similarly, Fig. 7 and Fig. 8 shows logarithmic *CF* curves for HEVC encoded "City" and "Race Horses" video sequences. As one can see, choose of modulation depth almost follows the same manner, regardless of video sequence under question. The only difference is in threshold values, which depend on texture and motion of video sequence.

D. Video Quality Metric

To measure user's satisfaction level, the utility function is defined as below:

$$UF = PSNR_{dec} \times R_{dec} \quad (14)$$

where $PSNR_{rec}$ is average peak signal to noise ratio of the decoded frames and R_{dec} is the decodable rate. The decodable rate is the ratio of the number of successfully decoded frames over the total number of frames [25]. Utility function takes both spatial video quality and availability of reconstructed frame. In the case of video transmission, quality of received video is a critical factor. It might be an unusable reconstructed frames when PSNR value is lower than a threshold. On the
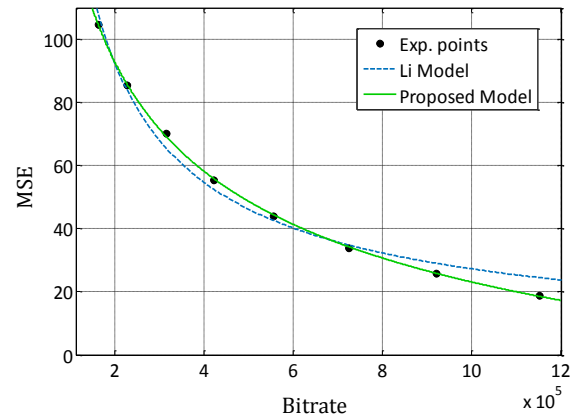

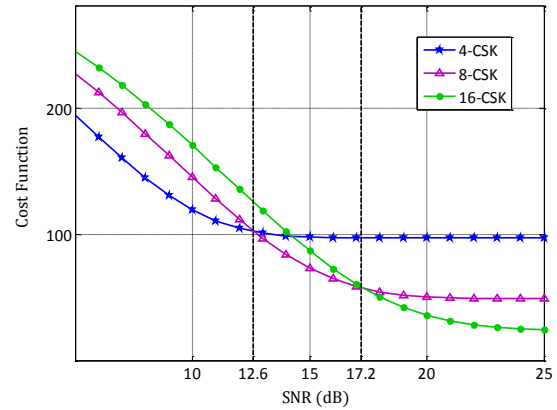Fig. 5. Fitting capability comparison of Li model and proposed model.

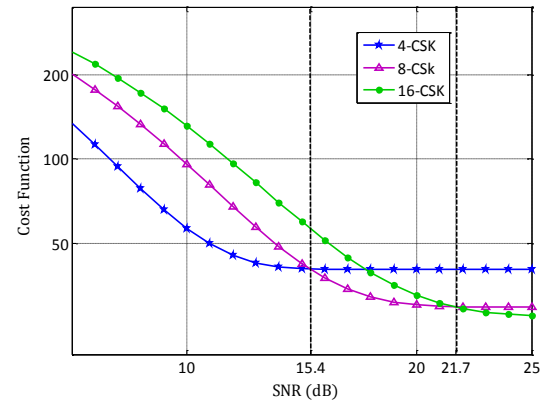Fig. 6. Cost Function for M = 4, 8 and 16 versus SNR; "Bus" video sequence.

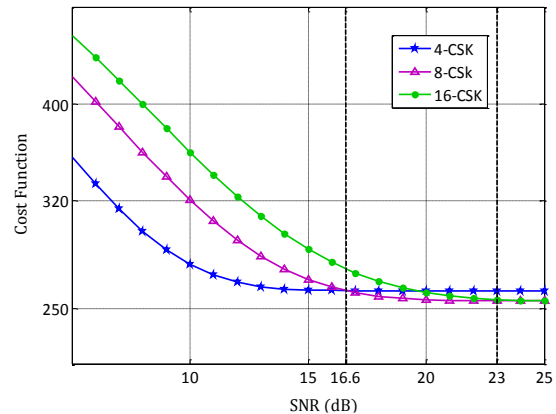Fig. 7. Cost Function for M = 4, 8 and 16 versus SNR; "City" video sequence.

Fig. 8. Cost Function for M = 4, 8 and 16 versus SNR; "Race Horses" video sequence.

other hand, number of reconstructed frames, indicates temporal quality of video. Consider a case, when you are watching a video sequence with noisy or dropped frames between high quality frames. This leads to an undesirable quality of experience. Therefore, both spatial and temporal video qualities are considered to achieve a reasonable metric for video quality. Higher value of utility function for a specified SNR value, means that there is a good video experience in terms of temporal and spatial quality. On the other hand, lower value of utility function could be the result of higher frame loss, lower PSNR or both of them which makes an undesirable quality of experience.

IV. RESULTS AND DISCUSSION

We first investigate the performance of proposed adaptive modulation scheme on the quality of the reconstructed video. Similar to other predictive encoders, HEVC has two basic modes namely intra mode and inter mode. These modes have different characteristics in terms of compression ratio and sensitivity to noise. Therefore, next, we examine the proper mode of HEVC to be used in VLC networks.

A. Video Quality for Proposed Adaptive CSK Modulation

Here we investigate the performance of proposed adaptive modulation scheme on the quality of reconstructed video using both utility function of (14) and subjective quality of reconstructed videos. Monte Carlo simulation is performed to get the utility function curves for three video sequences. Fig. 9 shows the utility function of "Bus" video sequence for 4-CSK, 8-CSK, 16-CSK and adaptive modulation cases versus different values of SNR. According to the given results in Fig. 6, adaptive modulation should switch from 4-CSK to 8-CSK after SNRs about 12.6 dB. The utility function curve for adaptive modulation represent benefits of proposed method. The utility function for 4-CSK is higher than adaptive modulation during SNRs of 12 dB to 16 dB interval. Additionally, for SNRs higher than 16 dB, utility function of 4-CSK is same as adaptive modulation, but switching to 8-CSK after 12.6 dB SNR in adaptive modulation provides 1.5x data rate which provides an opportunity to service further users. The simulation results show that 16-CSk has not qualified to video services over VLC network, at least for SNRs under question. Likewise, Fig. 10 and Fig. 11 shows the utility function curves for "City" and "Race Horses" video sequence, respectively. Simulation results indicate the proper performance of proposed algorithm considering both successful reconstruction of frames and spatial quality of them.

Furthermore, in order to provide some visual results, Fig. 12 shows a sample of reconstructed frames for constant modulation depth and adaptive modulation cases for "Bus" video sequence. From Fig. 12 it is evident that using a constant value of modulation depth results in distortion and artifacts which make video delivery meaningless. However, proposed algorithm switches to a proper modulation depth which results in a good subjective quality for the same SNR value and channel conditions. Similar results are obtained for "City" video sequence. As demonstrated is Fig. 13, proposed algorithm results in better subjective video
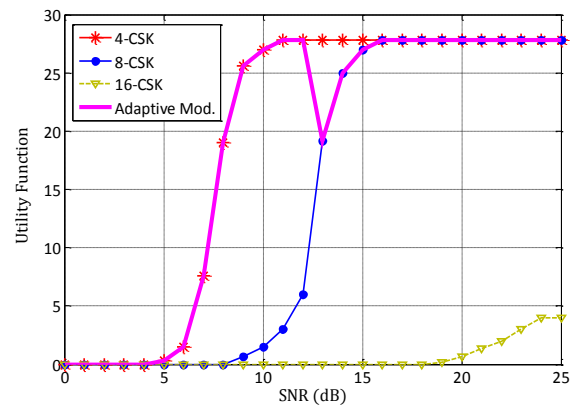

Fig. 9. Utility function for 4-CSK, 8-CSK, 16-CSK and adaptive modulation; "Bus" video sequences.
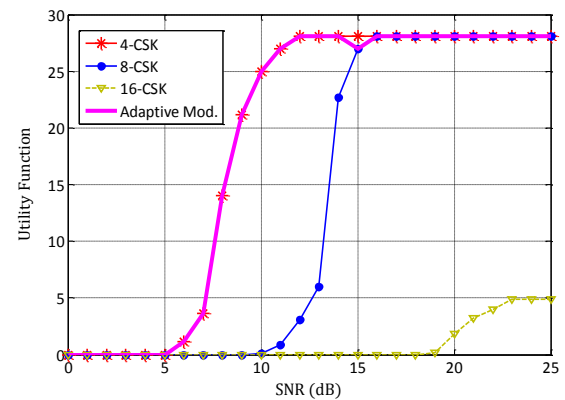

Fig. 10. Utility function for 4-CSK, 8-CSK, 16-CSK and adaptive modulation; "City" video sequences.
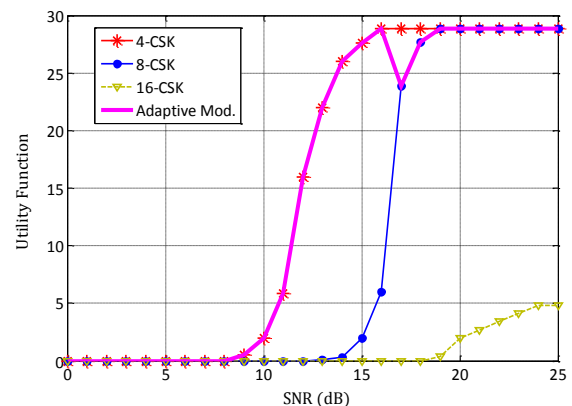

Fig. 11. Utility function for 4-CSK, 8-CSK, 16-CSK and adaptive modulation; "Race Horses" video sequences.

quality against constant modulation depth with the same amount of data rate.

B. Inter VS Intra

In predictive video encoding, there are three types of video frames based on prediction structure. Intra encoded (*I*) frames use only blocks contained within the current frame for prediction. Predicted (*P*) frames uses blocks within both the current frame and previously encoded *I* or *P* frame. Bidirectional (*B*) frames are predicted from blocks within the current frame and both previous and next *I* or *P* frame. Various combinations of *I*, *P* and *B* frames, results in different computational complexity and compression ratio for the HEVC encoder.

(a)

(b)   (c)

Fig. 12. Screenshot comparison for "Bus" video sequence; (a) original sequence, (b) noisy video sequence transmitted and reconstructed with adaptive modulation case, (c) noisy video sequence transmitted and reconstructed with constant modulation depth.
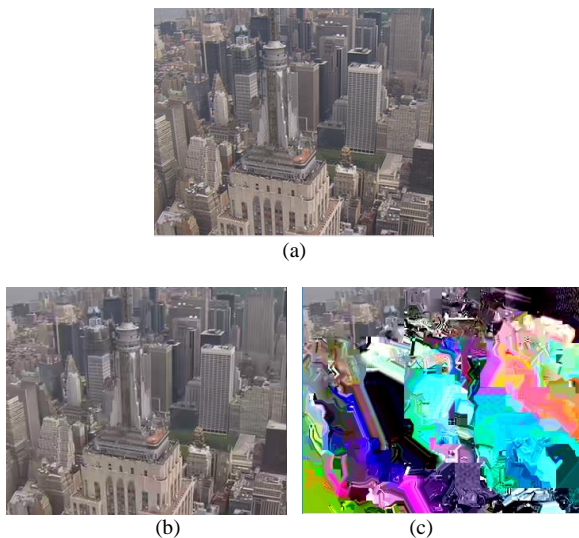

(a)

(b)   (c)

Fig. 13. Screenshot comparison for "City" video sequence; same order as Fig.12.

Intra mode of HEVC uses only *I* frames in coding structure. *I* frames do not exploit temporal redundancy which reduces compression ratio of intra mode. Due to the use of current frame for compression, reconstruction of each frame of intra mode only depends on itself. It means that in the case of occurrence any errors in a frame, this error will be limited to the corresponding frame. On the other hand, excluding motion estimation and compensation as the most complex task of predictive video coding, results in low computational complexity for intra mode of HEVC.

Inter mode of HEVC uses all type of video frames. Due to exploiting temporal redundancy through motion estimation and compensation, inter mode of HEVC has higher compression ratio and higher computational complexity compared to intra mode. Furthermore, *I* frames of the encoded video sequence can be reconstructed independently, however, reconstruction of *P* and *B* frames is dependent on the related reference frames. Therefore, every single error within the current

frame will propagate to all related frames. Hence, inter mode of HEVC is more vulnerable to noise than intra mode. Fig. 14 compares utility function of (14) using
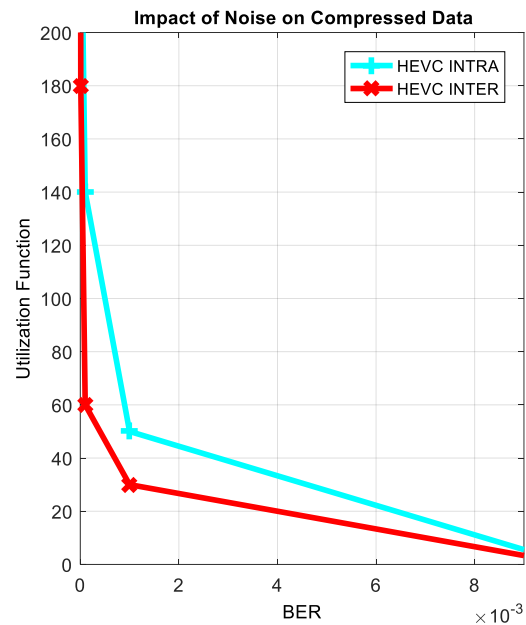

Fig. 14. Utility function for "City" video sequence encoded by HEVC Intra and Inter modes using proposed adaptive modulation.

inter and intra modes of HEVC for "City" video sequence. Similar results were obtained for other video sequences. As one can see, HEVC intra has better performance against noise compared to inter mode. Therefore, using HEVC intra results in better spatial and temporal quality.

However, UF only shows quality of reconstructed video without considering compression ratio. As mentioned, inter mode of HEVC has higher compression ratio than intra mode. This means that in a noiseless environment, inter mode results in lower bitrate than intra mode in similar video quality. In order to investigate compression capability of HEVC modes, we have compared rate-distortion (RD) performance of these modes. Fig. 15 shows RD curves of HEVC intra and inter modes for "City" video sequence. Considering RD curves of Fig. 15, has superior performance in the case of rate distortion performance. Similar results are obtained for other video sequences.

Considering results of Fig. 14 and Fig. 15, each mode of HEVC has its own merits and demerits. In higher SNR values, both inter and intra modes have desirable video quality in terms of UF of (14). Considering higher compression ratio of inter mode, it is the proper choice for this range since it provides to service further users without loss of temporal and spatial quality. However, in lower SNR values, intra mode is suggested because of providing higher video quality. Note that, using inter mode to provide more service in this range, wastes bandwidth completely due to the poor quality of experience.

V. CONCLUSION

In this study, an adaptive modulation scheme is proposed for proper video transmission over visible light communication network. This scheme considers the dependency of encoded video quality and
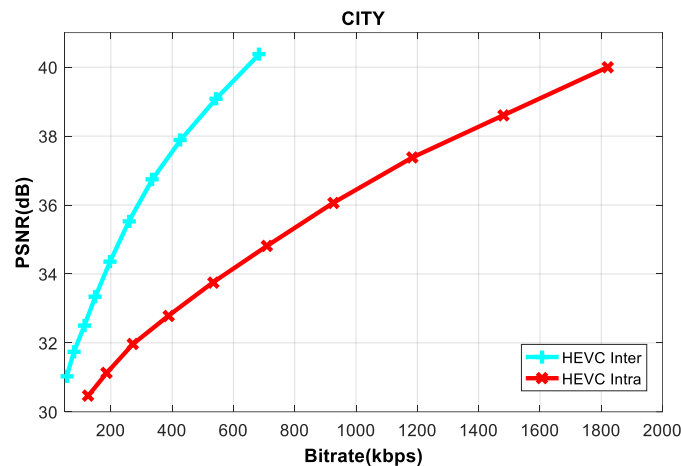
Fig. 15. Comparison of RD performance of HEVC Intra and Inter modes; "City" video sequence.

modulation BER to color shift keying modulation depth. This algorithm jointly minimizes BER and encoded video distortion via adaptive CSK modulation to decline frame loss besides desirable video quality. A utility function is defined to investigate the performance of proposed algorithm compared to the constant modulation depth video transmission case. The simulation results show superior performance of the proposed method in terms of the quality of experience. Additionally, in order to proper use of HEVC in V LC network, inter and intra modes are compared based on reconstructed video quality in noisy environments and RD performance. This comparison results in guidelines which facilitate choose of best HEVC mode for video delivery in VLC networks.

REFERENCES

[1] S. Pergoloni, M. Biagi, S. Rinauro, S. Colonnese, R. Cusani, and G. Scarano, "Merging Color Shift Keying and complementary Pulse Position Modulation for visible light illumination and communication," *Journal of Lightwave Technology,* vol. 33, pp. 192-200, 2015.

[2] R. Singh, T. O'Farrell, and J. P. David, "An enhanced color shift keying modulation scheme for high-speed wireless visible light communications," *Journal of Lightwave Technology,* vol. 32, pp. 2582-2592, 2014.

[3] R. Singh, T. O'Farrell, and J. P. David, "Performance evaluation of IEEE 802.15. 7 CSK physical layer," in *Globecom Workshops (GC Wkshps), 2013 IEEE,* 2013, pp. 1064-1069.

[4] S. Rajagopal, R. D. Roberts, and S.-K. Lim, "IEEE 802.15. 7 visible light communication: modulation schemes and dimming support," *Communications Magazine, IEEE,* vol. 50, pp. 72-82, 2012.

[5] B. Li, H. Li, L. Li, and J. Zhang, "λ Domain Rate Control Algorithm for High Efficiency Video Coding," *Image Processing, IEEE Transactions on,* vol. 23, pp. 3841-3854, 2014.

[6] L. Wu, Z. Zhang, J. Dang, and H. Liu, "Adaptive modulation schemes for visible light communications," *Journal of Lightwave Technology,* vol. 33, pp. 117-125, 2015.

[7] D. Han, K. Lee, and K. Lee, "Transmitting scalable video coding using VLC with color and dimming control to assure QoS," *Information Systems,* vol. 48, pp. 267-273, 2015.

[8] I. S. Association, "IEEE standard for local and metropolitan area networks-Part 15.7: short-range wireless optical communication using visible light," *IEEE Std,* vol. 802, pp. 7-2011, 2011.

[9] A. Halder and A. D. Barman, "Improved performance of colour shift keying using voronoi segmentation for indoor communication," in *Numerical Simulation of Optoelectronic Devices (NUSOD), 2014 14th International Conference on,* 2014, pp. 109-110.

[10] J. Rufo, J. Rabadan, F. Delgado, C. Quintana, and R. Perez-Jimenez, "Experimental evaluation of video transmission through LED illumination devices," *Consumer Electronics, IEEE Transactions on,* vol. 56, pp. 1411-1416, 2010.

[11] G. J. Sullivan, J.-R. Ohm, W.-J. Han, and T. Wiegand, "Overview of the high efficiency video coding (HEVC) standard," *Circuits and Systems for Video Technology, IEEE Transactions on,* vol. 22, pp. 1649-1668, 2012.

[12] J. Vanne, M. Viitanen, T. D. Hamalainen, and A. Hallapuro, "Comparative rate-distortion-complexity analysis of HEVC and AVC video codecs," *Circuits and Systems for Video Technology, IEEE Transactions on,* vol. 22, pp. 1885-1898, 2012.

[13] K. E. Psannis, "HEVC in wireless environments," *Journal of Real-Time Image Processing,* pp. 1-8, 2015.

[14] E. Sarbazi and M. Uysal, "PHY layer performance evaluation of the IEEE 802.15. 7 visible light communication standard," in *Optical Wireless Communications (IWOW), 2013 2nd International Workshop on,* 2013, pp. 35-39.

[15] D. Karunatilaka, F. Zafar, V. Kalavally, and R. Parthiban, "LED based indoor visible light communications: State of the art," *Communications Surveys & Tutorials, IEEE,* vol. 17, pp. 1649-1678, 2015.

[16] P. Das, Y. Park, and K.-D. Kim, "Performance improvement of color space based VLC modulation schemes under color and intensity variation, " *Optics Communications,* vol. 303, pp. 1-7, 2013.

[17] R. Kohno, "Project: IEEE P802. 15 Working Group for Wireless Personal Area Networks (WPANs)," *doc.: IEEE,* pp. 802.15-03, 2004.

[18] P. H. Pathak, X. Feng, P. Hu, and P. Mohapatra, "Visible Light Communication, Networking, and Sensing: A Survey, Potential and Challenges," *Communications Surveys & Tutorials, IEEE,* vol. 17, pp. 2047-2077, 2015.

[19] S. Arnon, *Visible light communication*: Cambridge University Press, 2015.

[20] M. K. Simon and M.-S. Alouini, *Digital communication over fading channels* vol. 95: John Wiley & Sons, 2005.

[21] Y. Sun, D. K. Borah, and E. Curry, "Optimal Symbol Set Selection in GSSK Visible Light Wireless Communication Systems," *Photonics Technology Letters, IEEE,* vol. 28, pp. 303-306, 2016.

[22] J. Jiang, R. Zhang, and L. Hanzo, "Analysis and Design of Three-stage Concatenated Colour-Shift Keying," *IEEE Transactions on Vehicular Technology,* vol. 64, pp. 5126-5136, 2014.

[23] M. Abdollahzadeh, H. Alizadeh Ghazijahani, and H. Seyedarabi, "Quality Aware HEVC Video Transmission Over Wireless Visual Sensor Networks," presented at the 2016 24th Iranian Conference on Electrical Engineering (ICEE), 2016.

[24] H. Alizadeh Ghazijahani, M. Abdollahzadeh, H. Seyedarabi, and M. J. Musevi Niya, "Adaptive CSK Modulation Guaranteeing HEVC Video Quality Over Visible Light Communication Network," presented at the 2016 8th International Symposium on Telecommunications (IST'2016), 2016.

[25] L. Cai, S. Xiang, Y. Luo, and J. Pan, "Scalable modulation for video transmission in wireless networks," *Vehicular Technology, IEEE Transactions on,* vol. 60, pp. 4314-4323, 2011.

Hamed Alizadeh Ghazijahani received his B.Sc. and M.Sc. degrees in electrical engineering from university of Tabriz, Iran in 2010 and 2013, respectively. He is currently Ph.D. candidate at University of Tabriz, Iran. His main research interests include video communication, optical and wireless communication systems and networks.

Milad Abdollahzadeh received his B.Sc. and M.Sc. degrees in electrical engineering from university of Tabriz, Tabriz, Iran where he is currently working toward the Ph.D. degree. His research interests include image and video processing, video compression, multimedia communication and signal processing for communication networks.

Hadi Seyedarabi received his B.Sc. degree from University of Tabriz, Iran, in 1993, the M.Sc. degree from K.N.T. University of technology, Tehran, Iran in 1996 and his Ph.D. degree from University of Tabriz, Iran, in 2006 all in Electrical Engineering. He is currently an associate professor of Faculty of Electrical and Computer Engineering in University of Tabriz, Tabriz, Iran. His research interests are Image Processing, Computer Vision, Video Coding, Human-Computer Interaction, Facial Expression Recognition and Facial Animation.

Javad Musevi Niya was born in Ahar, Iran. He received his B.Sc. degree from the University of Tehran and his M.Sc. and Ph.D. Degrees both in communications from Sharif University of Technology (SUT) and the University of Tabriz, respectively. Since September 2006, he has been with the Faculty of Electrical and Computer Engineering of the University of Tabriz, where he is currently an Associate Professor. His current research interests include wireless communication systems, multimedia networks and signal processing for communication systems and networks.

IJICTR

This Page intentionally left blank.